

IOWA STATE UNIVERSITY

QUANTIFICATIONS OF THE TURBULENCE
CHARACTERISTICS IN THE WAKE OF AN
AIRFOIL BY USING A HOTWIRE ANEMOMETER
LABORATORY

AER E 344 - LAB 07 - QUANTIFICATIONS OF THE TURBULENCE
CHARACTERISTICS IN THE WAKE OF AN AIRFOIL BY USING A
HOTWIRE ANEMOMETER

SECTION 3 GROUP 3

MATTHEW MEHRTENS

JACK MENDOZA

KYLE OSTENDORF

GABRIEL PEDERSON

LUCAS TAVARES VASCONCELLOS

DREW TAYLOR

PROFESSOR

HUI HU, PhD

College of Engineering

Aerospace Engineering

Aerodynamics and Propulsion Laboratory

AMES, MARCH 2024

ABSTRACT

Using the low-speed wind tunnel at Iowa State University, we measured the velocity profile downstream of an airfoil to analyze the turbulent wake region for different angle of attack (AoA). To measure the velocity profile in the wake region, we used a hot wire anemometer positioned downstream of the airfoil. Unfortunately, our results differ wildly from the mathematical and hypothetical predictions. We expect this is caused by a problem in the hot wire setup and configuration.

CONTENTS

Contents	ii
List of Figures	iii
Glossary	iv
Acronyms	1
1 Introduction	2
2 Methodology	3
2.1 Apparatus	3
2.2 Procedures	3
2.3 Derivations	5
3 Results	7
4 Discussion	11
4.1 Wake Analysis	11
4.2 Sources of Error	12
4.3 Future Work	12
5 Conclusion	14
A Appendix A	16
A.1 Additional Apparatus Pictures	16
A.2 Additional Figures	18
B Appendix B	23
B.1 Lab7Analysis.m	23

LIST OF FIGURES

2.1	A photograph of the hot wire anemometer downstream of the airfoil. . .	3
2.2	A photograph of the data acquisition box.	4
2.3	A photograph of the adjustable knob used to change the angle of attack of the airfoil.	4
3.1	A graph of the boundary layer thickness vs distance from the leading edge.	7
3.2	A graph of the normalized air speed as a function of the position behind the airfoil at a four degree angle of attack.	8
3.3	A graph of the normalized air speed as a function of the position behind the airfoil at different angles of attack.	8
3.4	A graph of the turbulence intenssity as a function of the position behind the airfoil at a four degree angle of attack.	9
3.5	A graph of the single-sided amplitude spectrum inside and outside the wake at a four degree angle of attack.	9
A.1	Hot Wire Anemometer behind the airfoil in the test section.	16
A.2	Hot Wire Anemometer behind the airfoil in the test section.	17
A.3	Adjustable knob to change the angle of attack of the airfoil.	17
A.4	A graph of the single-sided amplitude spectrum inside and outside the wake at a eight degree angle of attack.	18
A.5	A graph of the single-sided amplitude spectrum inside and outside the wake at a twelve degree angle of attack.	18
A.6	A graph of the single-sided amplitude spectrum inside and outside the wake at a sixteen degree angle of attack.	19
A.7	A graph of turbulence intensity vs position.	19
A.8	A graph of turbulence intensity vs position.	20
A.9	A graph of turbulence intensity vs position.	20
A.10	A graph of normalized velocity vs position.	21
A.11	A graph of normalized velocity vs position.	21
A.12	A graph of normalized velocity vs position.	22

GLOSSARY

C_d	Dimensionless coefficient of drag. (p. 12)
U/U_e	Normalized air speed. (p. 11)
Y/δ	Normalized vertical position of the hot wire anemometer downstream of the airfoil. (p. 11)

ACRONYMS

AoA angle of attack. (*p. i, 3, 5, 8, 9, 11, 12, 18–22*)

FFT fast Fourier transform. (*p. 11*)

MATLAB MATrix LABoratory. (*p. 14*)

RMS root mean square. (*p. 5*)

INTRODUCTION

The hot-wire anemometer uses a thin wire that passes electric current through it to maintain a constant temperature. As flow passes over the wire, voltage loss is recorded, enabling the anemometer to determine the velocity of the flow. In this experiment, the anemometer is used to track the velocity of flow at various points in the flow behind an airfoil.

Using voltage measurements from the hot-wire anemometer, we will create a profile of the airfoil wake region. We will calculate the coefficient of drag, and compare this to the calculations done for Lab 5 and Lab 6. We will also estimate the boundary layer thickness for the airfoil wake region profiles, and compare these with theoretical values.

METHODOLOGY

2.1 Apparatus

An airfoil is positioned in the wind tunnel test chamber as seen in [Figure 2.1](#). Downstream of the airfoil is a hot wire anemometer. The data was collected by the data acquisition tool shown in [Figure 2.2](#) which reads the voltage data from the hot wire and saves it to a .txt file.

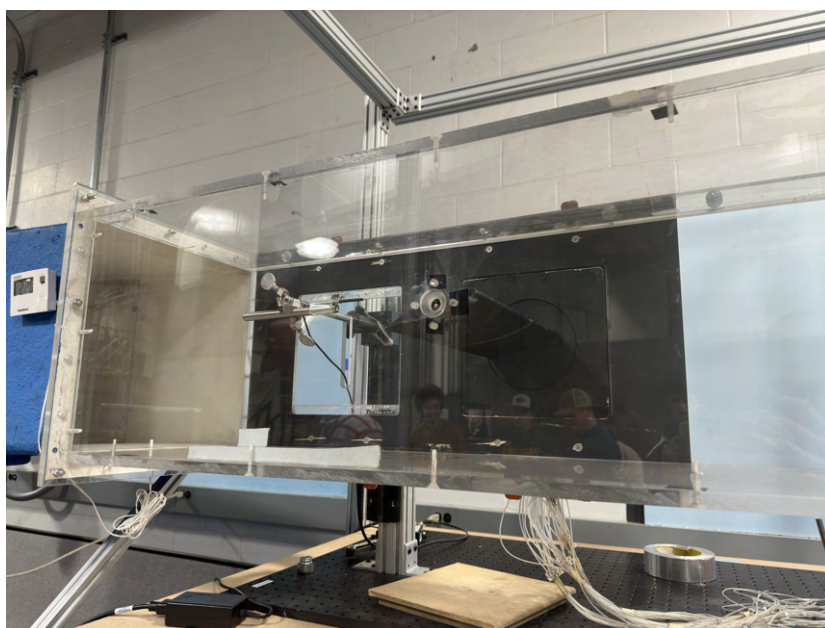


Figure 2.1: *The hot wire anemometer and the airfoil in the wind tunnel test chamber.*

When we collected the data at different heights, and we used the height adjustable knob to change the height as seen in [Figure 2.3](#)

2.2 Procedures

1. Set the wind tunnel motor speed to 15 Hz. Wait for the flow to stabilize.
2. Set the AoA to 4° .

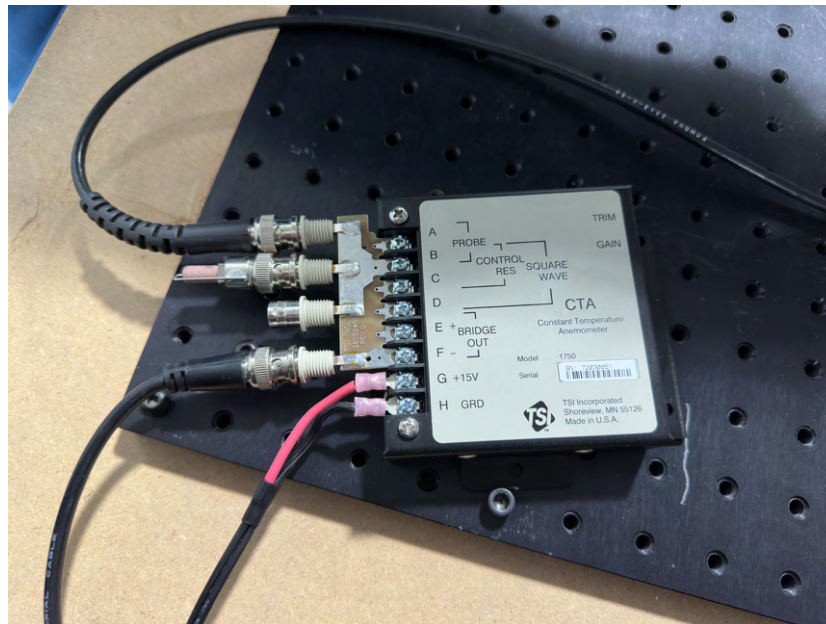


Figure 2.2: The data acquisition box which is connected to the hot wire anemometer and the data acquisition computer.



Figure 2.3: The adjustable knob used to change the angle of attack of the airfoil.

3. Vertically move the hot wire anemometer from 0 in. to 4 in. in 0.2 in. increments.
4. After each adjustment, acquire and save the data to a .txt data file.
5. Repeat Steps 3–4 using the following AoAs: 4, 8, 12 and 16.
6. Save the data to a flash drive for post-lab analysis.

2.3 Derivations

The turbulence intensity is found using the root mean square (RMS) of the velocity fluctuations over the mean velocity. (Hu, 2024) The mean velocity at each position around the airfoil is determined with the voltage data from the anemometer and the calibration polynomial from lab six in the form of Equation 2.1. The full calibration polynomial from lab six is Equation 2.2.

$$\bar{U} = C_0 + C_1\bar{v} + C_2\bar{v}^2 + C_3\bar{v}^3 + C_4\bar{v}^4 \quad (2.1)$$

$$\bar{U} = -10\,248.1714 + 34\,446.6867\bar{v} - 43\,230.9413\bar{v}^2 + 24\,021.8937\bar{v}^3 - 4982.7570\bar{v}^4 \quad (2.2)$$

The derivative of the calibration polynomial equation with respect to the mean voltage multiplied by the manometer voltage RMS will give the RMS of the velocity fluctuations at each position of the manometer around the airfoil (see Equation 2.3). Finally, the turbulence intensity is calculated in Equation 2.4.

$$u_{\text{rms}} = \left. \frac{\partial \bar{U}}{\partial v} \right|_{\bar{v}} = \left[C_1 + 2C_2\bar{v} + 3C_3\bar{v}^2 + 4C_4\bar{v}^3 \right] v_{\text{rms}} \quad (2.3)$$

$$TI = u_{\text{rms}}/\bar{U} \quad (2.4)$$

The momentum thickness is related to the coefficient of drag through equation Equation 2.6. However, the momentum thickness must first be calculated through Equation 2.5. In this lab, the integral was determined using the midpoint Riemann sum starting behind the surface of the airfoil and ending at the lowest position of the anemometer. The distance between each anemometer measurement was 0.2in.

$$\theta = \int_0^Y \frac{u}{U_e} \left(1 - \frac{u}{U_e} \right) dy \quad (2.5)$$

$$C_d = \frac{2\theta}{L} \quad (2.6)$$

The vortex shedding frequency graphs were created by taking the raw voltage data at two positions of each angle of attack, one inside the wake and one outside. A fast Fourier Transform of the raw data with a sampling frequency of 10 000 Hz is used to graph a single-sided amplitude spectrum and in the hopes of finding the vortex shedding frequency.

The following equations (Equation 2.7 and Equation 2.8) are theoretical estimations of the boundary layer thickness at a distance x over a flat plate.

$$\frac{\delta}{x} = \frac{5.0}{\sqrt{\text{Re}_x}} \quad (2.7)$$

$$\frac{\delta}{x} = \frac{0.37}{\text{Re}_x^{\frac{1}{5}}} \quad (2.8)$$

RESULTS

Figure 3.1 shows the theoretical boundary layer thickness as a function of the distance from the leading edge of a hypothetical flat plate using Equation 2.7 and Equation 2.8.

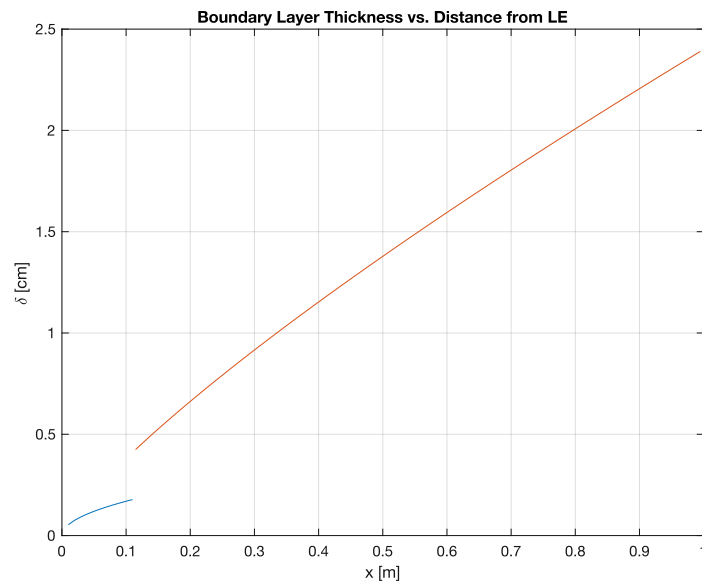


Figure 3.1: The boundary layer thickness as a function of the distance from the leading edge of a theoretical flat plate.

Figure 3.2 shows the relationship between fluid velocity normalized against the free stream velocity and the distance away from the surface of the airfoil normalized with the estimated boundary layer thickness from Figure 3.3. The minimum normalized fluid velocity is located behind the airfoil surface.

Figure 3.5 shows the single sided amplitude, where the data inside the wake is at a Y/δ of 0 and the data outside the wake is from the lowest possible position by the anemometer below the airfoil.

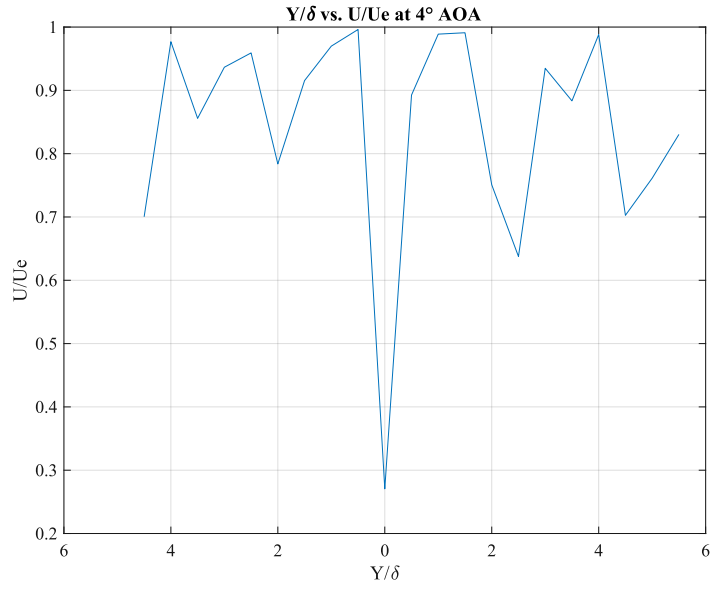


Figure 3.2: The normalized air speed as a function of the vertical position behind the airfoil at 4° AoA.

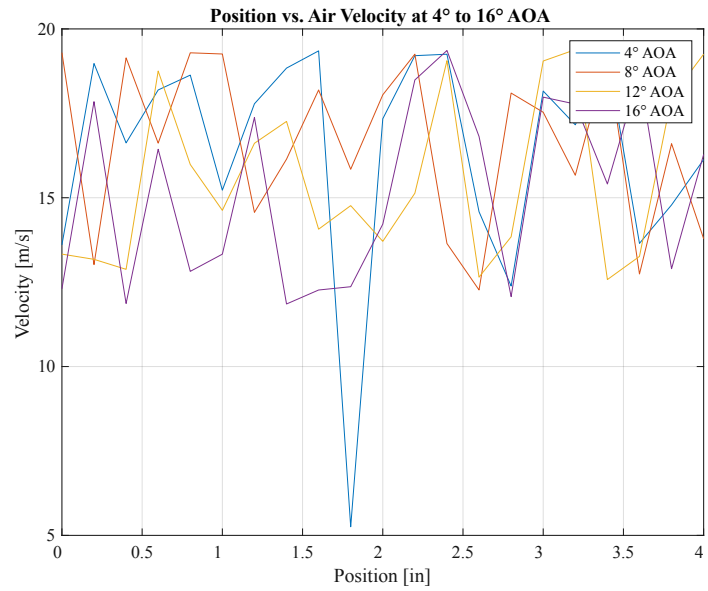


Figure 3.3: The normalized air speed as a function of the vertical position behind the airfoil at 4° to 16° AoAs.

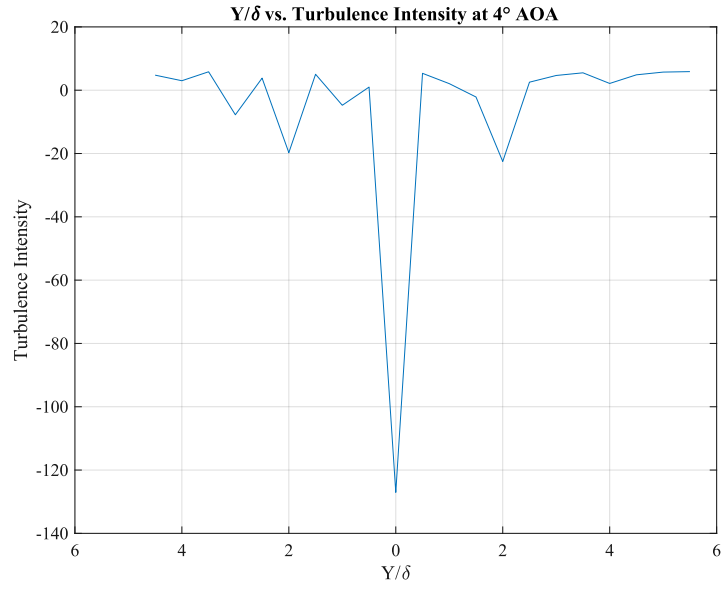


Figure 3.4: The turbulence intensity as a function of the vertical position behind the airfoil at 4° AoA.

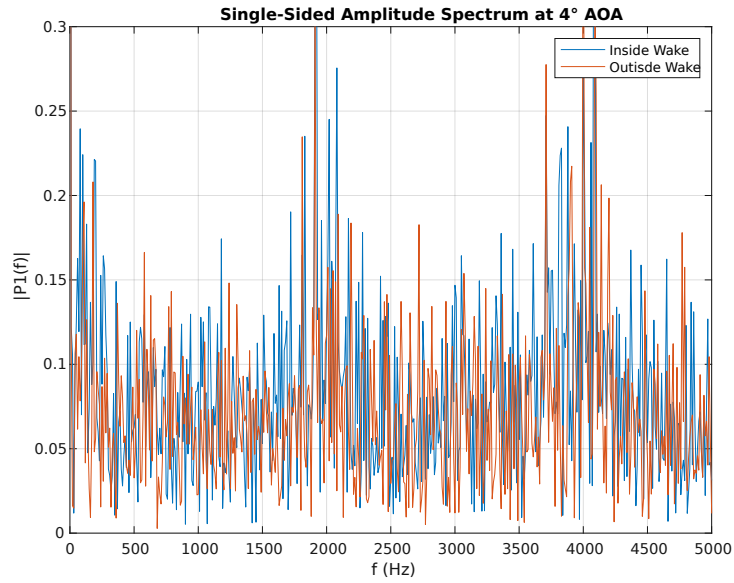


Figure 3.5: The single-sided amplitude spectrum inside and outside the wake region at a 4° AoA.

The C_d calculated at each angle of attack from Equation 2.6 is as follows:

$$4^\circ = 0.1277$$

$$8^\circ = 0.1371$$

$$12^\circ = 0.1469$$

$$16^\circ = 0.1359$$

Using Equation 3.1 and the subsequent parameters, we find the Reynolds number of about 1.322×10^5 for the airfoil wake measurements.

$$Re = \frac{\rho VL}{\mu} \quad (3.1)$$

$$\rho = 1.225 \text{ kg/m}^3$$

$$\mu = 18.18 \times 10^{-6} \text{ Pa s}$$

$$L = 0.101 \text{ m}$$

$$V = 19.4 \text{ m/s}$$

$$Re = 1.322 \times 10^5$$

DISCUSSION

4.1 Wake Analysis

The data in our lab is clearly erroneous. The sources of this error are discussed in more detail in [Section 4.2](#). Beginning with the Y/δ vs. U/U_e graph shown in [Figure 3.2](#), we see the shape generally matches our theoretical expectations, although the region outside the wake, where we would expect the flow to be laminar, is far less uniform than we measured in previous labs. This is only exacerbated when we increase the angle of attack as shown in the additional Y/δ vs. U/U_e graphs in [Section A.2](#). At AoAs above 4° , the wake region disappears completely, implying either instrumentation error or that the wake region covers the entire width of measurements gathered. Since the boundary layer thickness we estimated in pre-lab (see [Figure 3.1](#)) was on the scale of 0 cm to 2.5 cm, although it is possible, it seems unlikely the wake region exceeded the 0 in. to 4 in. range we measured downstream of the airfoil. As seen in [Figure 3.3](#), the measurements taken with an AoA above 4° seem to have no correlation whatsoever and look more like noise. Even the 4° AoA measurements may have been coincidental noise.

[Figure 3.4](#) shows the turbulence intensity profile downstream of the airfoil at an AoA of 4° . Based on the example results we were shown prior to the lab, these turbulence intensity values should have generally been a reflection of the velocity profile—*i.e.*, when the velocity in the wake was at a low, the turbulence intensity should have been at a high—and they should have been positive values in the range of 2 to 3. [Figure 3.4](#) has neither the appropriate shape, magnitude, nor sign, and the turbulence intensity graphs for the higher AoAs (see [Section A.2](#)) are no better. Again, the reason for this is discussed in greater detail in [Section 4.2](#), but we suspect this error is compounded by an invalid hot wire calibration polynomial.

The spectrum analysis in [Figure 3.5](#) is equally meaningless. There do appear to be significant spikes around 2000 Hz and 4000 Hz, perhaps implying there was some type of vortex shedding or turbulent behavior occurring. But to assume that were true would ignore the obvious lack of correlation over the entire frequency spectrum. The fast Fourier transform (FFT) looks far more like random noise. In the examples we observed prior to the lab, at low angles of attack, the FFT should have been fairly unexcited, which

is obviously not what our data shows.

The Reynolds Number calculation is reasonable considering the free stream velocity value was determined using the lab two motor frequency vs air speed relationship. Despite the unreliable data from the anemometer, the coefficient of drag at each angle of attack almost follows the expected trend. As the angle of attack increases, the C_d would increase. The C_d does increase for angles of attack from 4° to 12° , but then decreases at an AoA of 16° . Since the data is unreliable, as discussed in [Section 4.2](#), this is likely a coincidence.

4.2 Sources of Error

For our data to be this deviant from the theoretical predictions, we must assume there were significant sources of error in the experimental setup, data analysis, or both. While we absolutely cannot vouch for our analysis with complete certainty—we would need more time to validate our calculations on different data sets—we expect the most significant error come from two sources: the hot wire setup and our hot wire calibration polynomial.

Any number of factors could have affected the hot wire data. just to name a few potential sources of error: the electrical wires connected to the hot wire apparatus may have had a loose connection at either terminal; there may have been some type of electromagnetic radiation causing noise or interference on the wires; the hot wire apparatus may have been broken, misaligned, or had a short. It is also possible the data acquisition software was misconfigured, although, we would expect this to result in data of the wrong order of magnitude, not the wrong shape entirely. A mechanical flaw in the apparatus is more likely given the random nature of the data we collected. Throughout the data, there are segments that seem reasonable—*e.g.*, the 4° AoA data—but in general, the data seems to have had significant noise added into it.

In addition to the noisy data, our hot wire calibration polynomial may be invalid for this hot wire anemometer. When exploring potential problems in our analysis script, we tried using the hot wire calibration polynomial calculated by a different group in our section, and we found our turbulence intensity graphs changed shape and magnitude significantly. Although they did not mirror our velocity profiles as expected, they did at least become positive.

4.3 Future Work

Due to the potentially erroneous hot wire data or calibration data, we were unable to analyze the wake region of the airfoil. We also cannot prove definitively the source of our error, but we think it is most likely due to noise in the hot wire anemometer apparatus. To improve our results, we would take the following corrective measures:

1. Test our analysis script on a set of a reliable data and compare the results to the

expected values—fixing bugs and making changes as necessary.

2. Re-calibrate and verify the functionality and accuracy of the hot wire anemometer apparatus.
3. Confirm the settings in the data acquisition software and repeat the experimental data collection.

CONCLUSION

To analyze the flow patterns downstream of an airfoil, we measured the velocity profile downstream of the airfoil using a hot wire anemometer. Due to erroneous data collected from the hot wire anemometer or a misconfiguration of the hot wire anemometer, we were unable to generate a conclusive analysis of the wake region. To rectify this and generate proper results, we would thoroughly review the MATLAB analysis script and, if necessary, validate the functionality and accuracy of the hot wire anemometer before repeating the experiment.

BIBLIOGRAPHY

Hu, Hui (2024). *Quantifications of the Turbulence Characteristics in the Wake of an Airfoil by using a Hotwire Anemometer*. Iowa State University. URL: https://www.aere.iastate.edu/~huhui/teaching/2024-01S/AerE344/lab-instruction/AerE344L-Lab-07-instruction_hotwire-wake-measurement.pdf.

APPENDIX A

A.1 Additional Apparatus Pictures

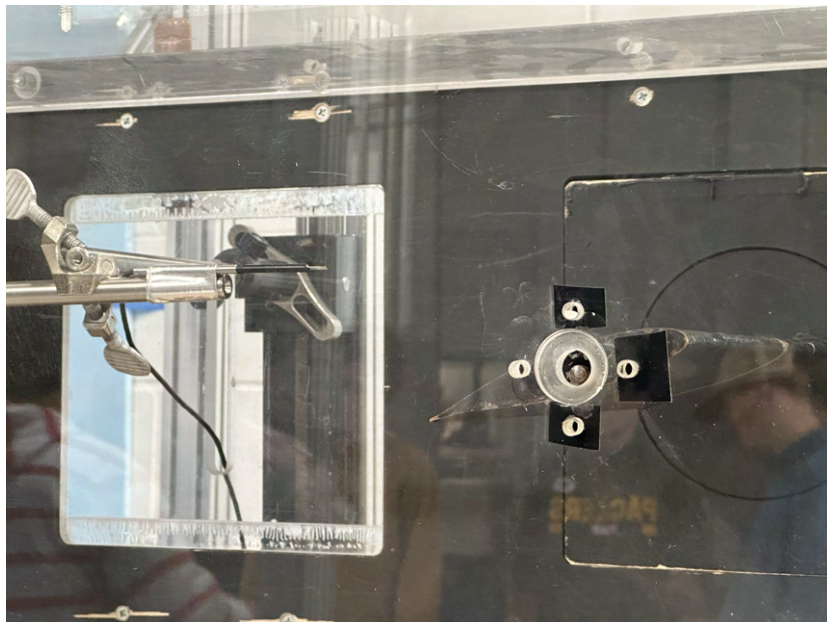


Figure A.1: *Hot Wire Anemometer behind the airfoil in the test section.*



Figure A.2: *Wire Anemometer behind the airfoil in the test section.*



Figure A.3: *Adjustable knob to change the angle of attack of the airfoil.*

A.2 Additional Figures

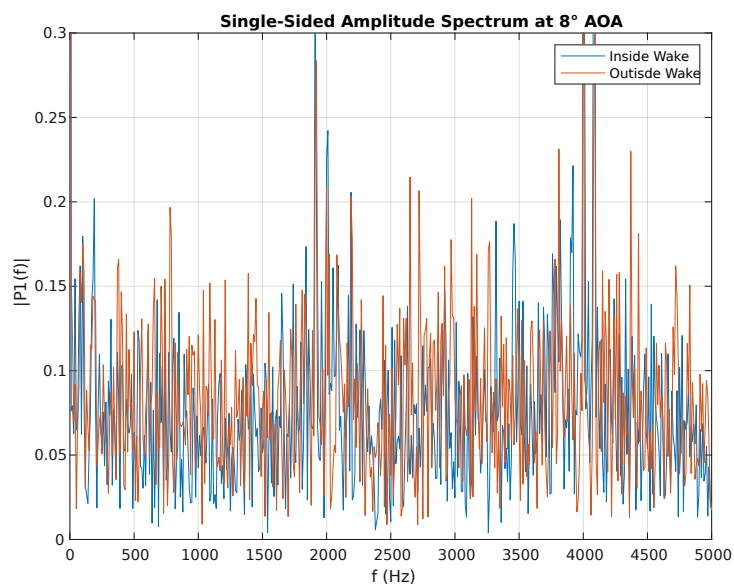


Figure A.4: The single-sided amplitude spectrum inside and outside the wake region at a 8° AoA.

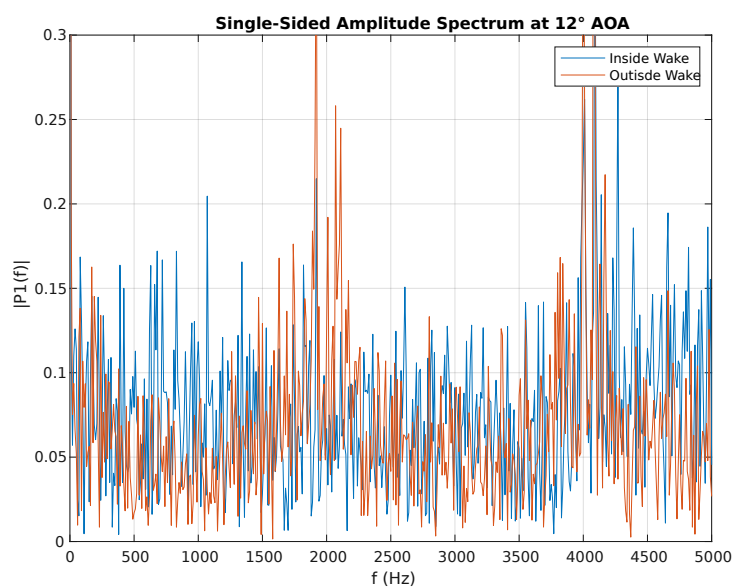


Figure A.5: The single-sided amplitude spectrum inside and outside the wake region at a 12° AoA.

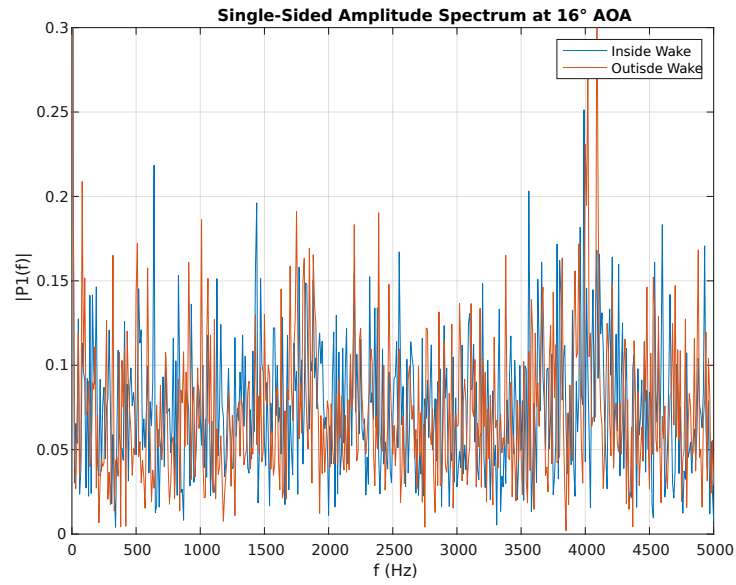


Figure A.6: The single-sided amplitude spectrum inside and outside the wake region at a 16° AoA.

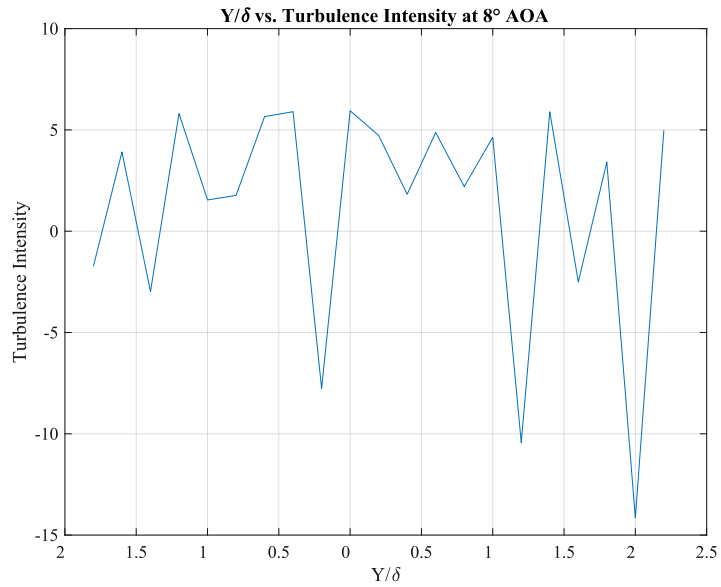


Figure A.7: Turbulence intensity at a 8° AoA.

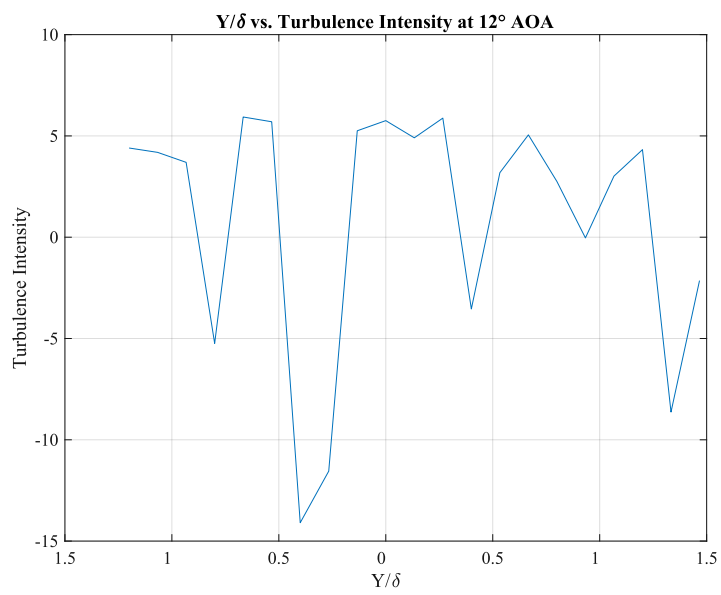


Figure A.8: *Turbulence intensity at a 12° AoA.*

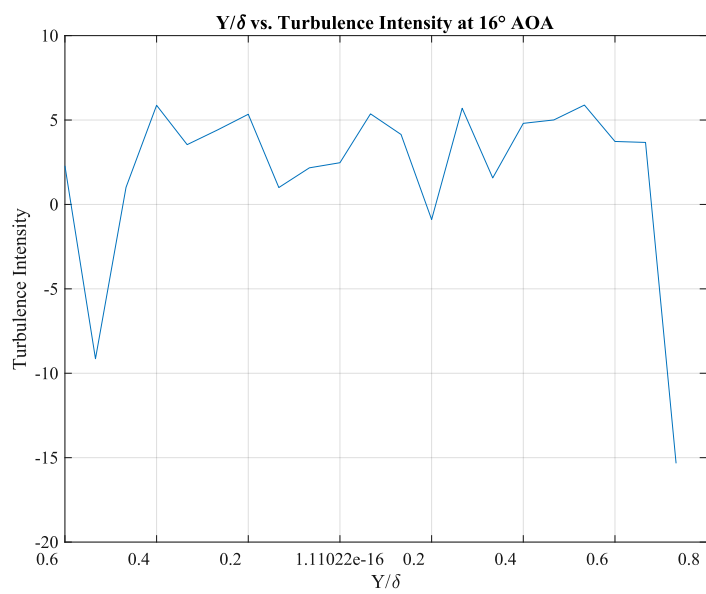


Figure A.9: *Turbulence intensity at a 16° AoA.*

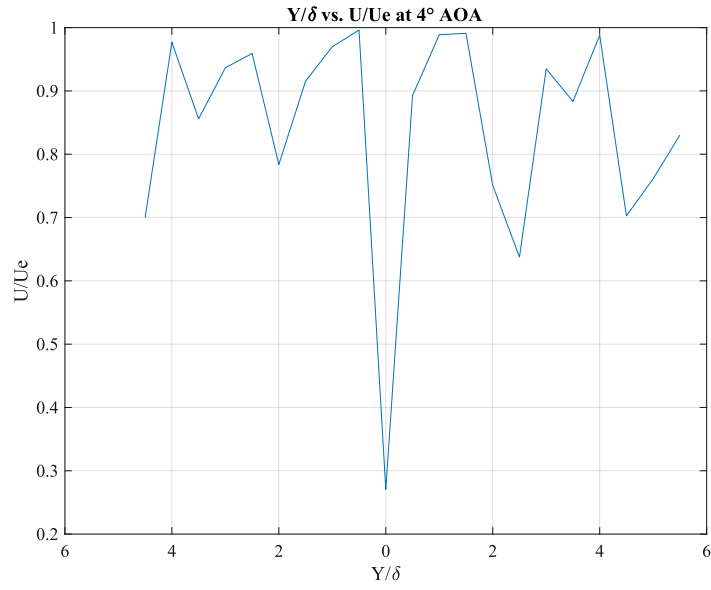


Figure A.10: Velocity at a 8° AoA.

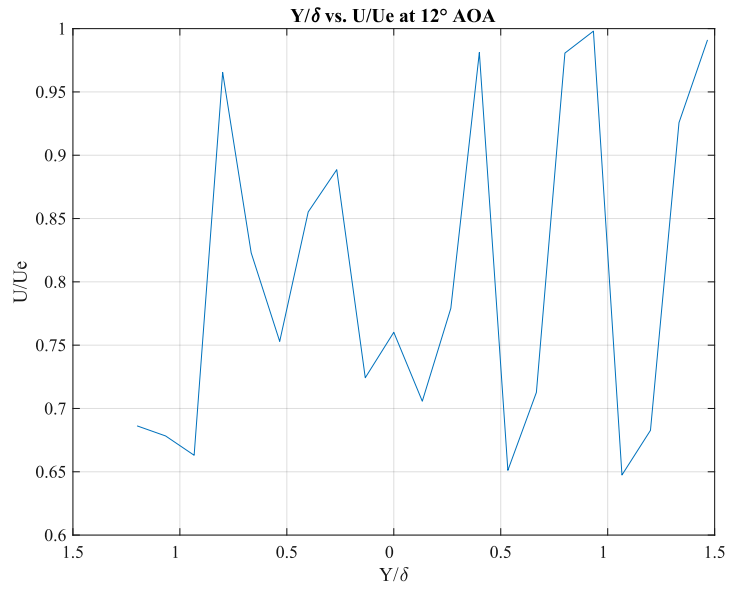


Figure A.11: Velocity at a 12° AoA.

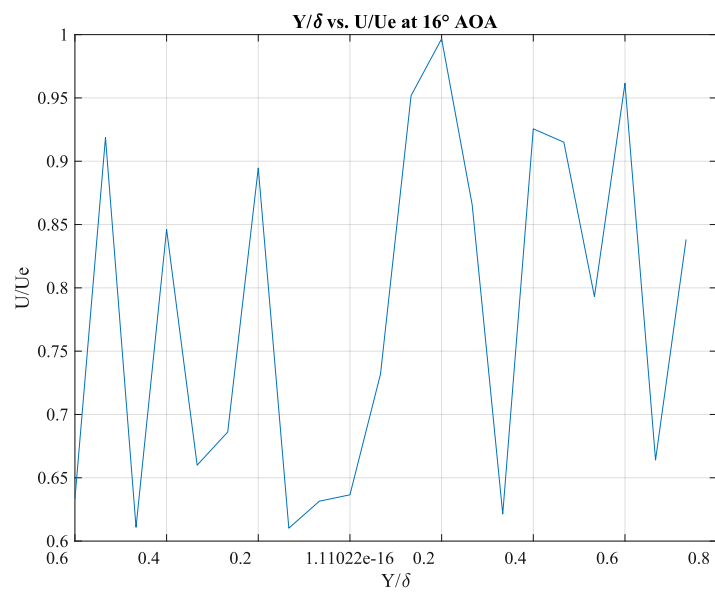


Figure A.12: *Velocity at a 16° AoA.*

APPENDIX B

B.1 Lab7Analysis.m

```

1  % AER E 344 Spring 2024 Lab 04 Analysis
2  % Section 3 Group 3
3  clear, clc, close all;
4
5  figure_dir = "../Figures/";
6  data_zip = "../data.zip";
7
8  %% Parameters
9  aoa = 4:4:16;
10 pos = 0:0.2:4;
11 figure_count = 1;
12
13 %% Constants
14 % Viscosity calculated at 21.2°C
15 % https://www.engineeringtoolbox.com/air-absolute-kinematic-viscosity-d\_601
16 % .html
17 mu_air = 18.18e-6; % [Pa*s]
18 rho_air = 1.225; % [kg/m^3]
19 L = 0.101; % [m]
20 % Curve fit equation for voltage (x) vs air speed (y) from Lab 6
21 v_vs_U = @(x) -4982.7570*x.^4 + 24021.8937*x.^3 + -43230.9413*x.^2 + 34446.6867*x +
    ↪ -10248.1714;
22 Cf = [34446.6867 -43230.9413 24021.8937 -4982.7570];
23 % v_vs_U = @(x) (6553.11832)*x.^4 + (-30178.43731)*x.^3 + (52087.72644)*x.^2 +
    ↪ (-39881.78843)*x + (11425.60699);
24 % Cf = [-39881.78843 52087.72644 -30178.43731 6553.1183];
25 row = length(aoa);
26 col = length(pos);
27 volt = zeros(row, col); % [V] voltage
28 U = zeros(row, col); % [m/s] velocity
29 Ue = 1.32372*(15) -0.430966; % [m/s] Freestream velocity estimated from Lab 2
30 d_m = .2*.0254; % [m] Distance between measurements
31
32 %% Reynolds Number

```

```
33 Re = rho_air * Ue * L / mu_air;
34
35 %% Find avg. Voltage and Air Speed
36 unzip(data_zip);
37 for i = 1 : row
38     for j = 1 : col
39         name = "./" + aoa(i) + "/" + pos(j) + "in.txt";
40         temp = readmatrix(name);
41         volt(i, j) = mean(temp(4:1003,2));
42         U(i, j) = v_vs_U(volt(i, j));
43     end
44 end
45
46 %% Position vs. Velocity Graph
47 figure.figure_count
48 figure_count = figure_count+1;
49 for i = 1:row
50     plot(pos, U(i,:));
51     hold on
52 end
53 fontname("Times New Roman");
54 fontsize(12, "points");
55 title_str = "Position vs. Air Velocity at 4° to 16° AOA";
56 title(title_str);
57 xlabel("Position [in]");
58 ylabel("Velocity [m/s]");
59 grid on;
60 legend(aoa + "° AOA");
61 xticks = get(gca, 'XTick');
62 abs_xticks = abs(xticks);
63 set(gca, 'XTickLabel', abs_xticks);
64 saveas(gcf, figure_dir + "Position vs. Air Velocity at 4 to 16 AOA.svg");
65
66 %% Position vs. Voltage Graph
67 % figure.figure_count;
68 % figure_count = figure_count+1;
69 % for i = 1:row
70 %     plot(pos, volt(i,:));
71 %     hold on
72 % end
73 % fontname("Times New Roman");
74 % fontsize(12, "points");
75 % title_str = "Position vs. Anemometer Voltage at 4° to 16° AOA";
76 % title(title_str);
77 % xlabel("Position [in]");
78 % ylabel("Voltage [V]");
79 % grid on;
80 % legend(aoa + "° AOA");
81
82 % Boundry Layer determined from graph estimations (looking/making it up)
83 delta = [0.4, 1, 1.5, 3]; % [in]
```

```

84 delta_pos = 1.8; % [in] try to make position centered at wake
85 y_right = .2 : .2 : max(pos) - delta_pos;
86 y_left = min(pos) - delta_pos : .2 : 0;
87 y_pos = [y_left,y_right];
88
89 %% Normalized Position vs. Normalized Velocity Graph
90 y_delta = zeros(row,col);
91 U_Ue = zeros(row,col);
92 for i = 1:row
93     figure.figure_count
94     figure_count = figure_count+1;
95     y_delta(i,:) = y_pos/delta(i);
96     U_Ue(i,:) = U(i,:)/Ue;
97     plot(y_delta(i,:), U_Ue(i,:));
98     fontname("Times New Roman");
99     fontsize(12, "points");
100    title_str = "Y/\delta vs. U/Ue at " + aoa(i) + "° AOA";
101    title(title_str);
102    xlabel("Y/\delta");
103    ylabel("U/Ue");
104    grid on;
105    xticks = get(gca, 'XTick');
106    abs_xticks = abs(xticks);
107    set(gca, 'XTickLabel', abs_xticks);
108    saveas(gcf, figure_dir + "Ydelta vs. UUE at " + aoa(i) + " AOA.svg");
109 end
110
111 %% Normalized Position vs. Turbulence Intensity
112 turb_i = zeros(row,col);
113 for i = 1:row
114     v_rms = zeros(1,col);
115     for j = 1:col
116         % find rms of raw data at each position
117         name = "./" + aoa(i) + "/" + pos(j) + "in.txt";
118         temp = readmatrix(name);
119         v = temp(4:1003,2);
120         v_rms(j) = rms(v);
121     end
122     v_ = volt(i,:);
123     u_rms = (Cf(1) + 2*Cf(2)*v_ + 3*Cf(3)*v_.^2 + 4*Cf(4)*v_.^3).*v_rms;
124     turb_i(i,:) = u_rms./U(i,:);
125
126     figure.figure_count
127     figure_count = figure_count+1;
128     plot(y_delta(i,:), turb_i(i,:));
129     fontname("Times New Roman");
130     fontsize(12, "points");
131     title_str = "Y/\delta vs. Turbulence Intensity at " + aoa(i) + "° AOA";
132     title(title_str);
133     xlabel("Y/\delta");
134     ylabel("Turbulence Intensity");

```

```
135     grid on;
136     xticks = get(gca, 'XTick');
137     abs_xticks = abs(xticks);
138     set(gca, 'XTickLabel', abs_xticks);
139     saveas(gcf, figure_dir + "Ydelta vs. Turbulence Intensity at " + aoa(i) + "
        ↳ AOA.svg");
140 end
141
142 %% Vortex Shedding Frequency
143 for i = 1:4
144     figure_count = figure_count + 1;
145     figure_count = figure_count + 1;
146     % Inside Wake
147     name = "./" + aoa(i) + "/" + pos(10) + "in.txt";
148     temp = readmatrix(name);
149     y = temp(4:1003, 2);
150     Fs = 10000;
151     n = length(y);
152     Y = fft(y);
153     P2 = abs(Y/n); % Compute the two-sided spectrum
154     P1 = P2(1:n/2+1); % Compute the single-sided spectrum
155     P1(2:end-1) = 2*P1(2:end-1);
156     f = Fs*(0:(n/2))/n; % Define the frequency domain
157     % Plot the single-sided amplitude spectrum inside wake
158     plot(f, P1);
159     hold on
160
161     % Outside Wake
162     name = "./" + aoa(i) + "/" + pos(1) + "in.txt";
163     temp = readmatrix(name);
164     y = temp(4:1003, 2);
165     Fs = 10000;
166     n = length(y);
167     Y = fft(y);
168     P2 = abs(Y/n); % Compute the two-sided spectrum
169     P1 = P2(1:n/2+1); % Compute the single-sided spectrum
170     P1(2:end-1) = 2*P1(2:end-1);
171     f = Fs*(0:(n/2))/n; % Define the frequency domain
172     % Plot the single-sided amplitude spectrum inside wake
173     plot(f, P1);
174
175     title_str = "Single-Sided Amplitude Spectrum at " + aoa(i) + "° AOA";
176     title(title_str);
177     xlabel('f (Hz)');
178     ylabel('|P1(f)|');
179     ylim([0, .3]);
180     legend({'Inside Wake', 'Outside Wake'})
181     grid on;
182     saveas(gcf, figure_dir + "Single-Sided Amplitude Spectrum at " + aoa(i) + "
        ↳ AOA.svg");
183 end
```

```
184
185 %% Momentum Thickness
186 theta = zeros(1,row);
187 C_D = zeros(1,row);
188 for i = 1:row
189     for j = 10:20
190         f1 = U(i,j)/Ue*(1- U(i,j)/Ue);
191         f2 = U(i,j+1)/Ue*(1-U(i,j+1)/Ue);
192         theta(i) = theta(i) + d_m*((f1 + f2)/2);
193     end
194     C_D(i) = 2 * theta(i) / L;
195 end
196
197 %% Delete unzipped data
198 dirs = {'4', '8', '12', '16'};
199 for i = 1:length(dirs)
200     rmdir(dirs{i}, 's');
201 end
```
